Studies on the Regulation of the Pit2 Sodium Dependent Phosphate Transporter / Amphotropic Murine Leukemia Virus Receptor

PhD Thesis

Zsolt Jobbagy

Department of Medical Microbiology and Immunology
University of Szeged
6720 Szeged
Dóm tér 10
Hungary

Laboratory of Cellular Oncology
National Cancer Institute
National Institutes of Health
Bethesda MD, 20892
USA

Table of Contents

Introduction

The amphotropic murine leukemia virus (A-MuLV) has the ability to infect a variety of mammalian cell lines. This broad tropism together with its relatively simple organization has made this retrovirus a particularly promising vector for gene therapy. Although A-MuLV-derived vectors are now broadly used for gene therapy purposes (*Batra et al. 1998; Cardinali et a.l 1998; Yang et al. 1999*), little is known about the biology of their receptor. Cell surface receptors for A-MuLV have been cloned (*Miller et al. 1994; van Zeijl et al. 1994; Wilson et a.l 1995*) and demonstrated to serve as sodium-dependent phosphate (Na^+/P_i) transporters in the normal physiology of diverse cell types (*Kavanaugh et al. 1994, Wilson et al. 1995*). Based on their structural and functional characteristics, these molecules, together with the gibbon ape leukemia virus (GALV) receptor, were classified as type III Na^+/P_i transporters (*Kavanaugh and Kabat 1996*) and were designated Pit-2 and Pit-1, respectively (*Eiden et al. 1996, Kavanaugh et al. 1994*).

The activity and protein levels of the Pit-2 phosphate transporter/viral receptor are highly regulated in cells. Pit-2-mediated Na^+/P_i uptake can be specifically blocked by infection of cells with A-MuLV (*Wilson et al. 1995*), and expression of amphotropic envelope protein (Env) in murine cells also has been shown to inhibit phosphate transport (*Kavanaugh et al. 1994*). A similar loss of the Pit-1 transporter functions has been described for GALV-infected cells (*Olah et al. 1994*). Phosphate concentration changes also have been shown to regulate P_i uptake activity. Depletion of extracellular phosphate was found to increase Pit-2 and Pit-1 expression three- to fivefold in fibroblasts (*Kavanaugh et al. 1994*). Moreover, removal of phosphate from the culture media was shown to both increase the amount of Pit-2 mRNA and the quantity of a 71-kDa protein specifically recognized by antibodies against Pit-2. This increase in Pit-2 mRNA levels observed in response to P_i depletion appeared to be regulated not at a transcriptional but rather at a posttranscriptional level due to enhanced mRNA stability (*Chien et al. 1998*). In a study carried out with CHO cells, the levels of Pit-2 at the cell surface remained unchanged following variations of the phosphate supply, but the efficiency of phosphate uptake and retrovirus entry was found to be inversely related to

the extracellular phosphate concentration (*Rodrigues et al. 1999*). These results suggested that Pit-2 activities may be modulated by posttranslational modifications of the cell surface Pit-2 proteins in response to changes in phosphate concentration and that such modifications are required to activate phosphate transporter and retrovirus receptor functions.

Protein kinases, including members of the protein kinase C family, regulate numerous biological functions, including intracellular protein trafficking and the activities of different ion transporters (*Nishizuka et al. 1995*). Previously, it was shown that sodium-dependent phosphate (Na/P_i)[1] transport was stimulated by protein kinase C (PKC) and inhibited by protein kinase A in NIH 3T3 cells. Phorbol 12-myristate 13-acetate (PMA), an activator of PKC, was found to cause a rapid (within 10 min) stimulation of short term Na/P_i uptake (*Olah et al. 1993*). However, at that time the identity of the Na/P_i transporter stimulated in response to PMA was not known, and this prevented further characterization of the PKC-mediated activation of the transporter. More recently, cell surface receptors for the gibbon ape leukemia virus (Glvr-1 and Pit-1) and the amphotropic murine leukemia virus (Ram-1, Ear, and Pit-2) were demonstrated to serve as Na/P_i transporters in the normal cellular physiology of diverse cell types (*Kavanaugh et al. 1994; Olah et al. 1994; Wilson et al. 1995*). We have established in the presented studies that PMA treatment of cells enhances Na^+/P_i uptake via stimulation of Pit-2 and that this effect is specifically mediated through PMA activation of the PKCε isoform.

Cells infected by retroviruses display a strong resistance to superinfection by viruses that utilize the same receptor as the pre-infecting virus but retain susceptibility to viruses that use a different receptor. This phenomenon, termed superinfection interference, is thought to arise from interaction of the viral envelope protein with the receptor (*Coffin 1996*). However, the level and site of this interaction remain obscure. While superinfection and receptor down-regulation phenomena are widely recognized, and methods based on viral superinfection interference are commonly used in murine retrovirus research (*Eglitis et al. 1993; Miller and Wolgamot 1997*), the mechanisms underlying the loss of transporter and receptor functions are largely unknown (*Coffin 1996*). To determine the fate of Pit-2 in A-MuLV-producing infected and control uninfected cells, we constructed plasmids capable of efficiently expressing ε-epitope-

and green fluorescent protein (GFP)-tagged human Pit-2 proteins in mammalian cells. The results presented in this thesis demonstrate that the tagged Pit-2 receptors are localized to the plasma membrane in uninfected NIH 3T3 cells. However, when NIH 3T3 cells expressing these tagged proteins are infected with A-MuLV, the tagged receptors are no longer detectable in the plasma membrane but are found redistributed to punctate structures within the cytosolic compartment. This loss of Pit-2 viral receptors from the cell membrane apparently is responsible for superinfection interference induced with A-MuLV infection.

Amino acid sequence data obtained for the Pit-1 and Pit-2 receptor-transporters has revealed multiple sites potentially susceptible to phosphorylation by protein kinases, including PKC, which are found within the hydrophilic cytoplasmic domain of both transporters between residues 250 and 450. Indeed, parathyroid hormone-induced regulation of transporter function mediated through activation of protein kinase A and PKC has been described for type I and II Na/P_i transporters present in kidney brush-border membranes (*Chien et al. 1996*). In addition to parathyroid hormone, prostaglandin E2, insulin-like growth factor 1, and vitamin D_3 all have been reported to regulate Na/P_i uptake through activation of PKC in osteoblasts, another cell type that uses high levels of inorganic phosphate (*Coffin 1996; Eglitis et al 1993; Eiden et al. 1996*). It also has been suggested that a phospholipase C^{γ}-PKC signaling pathway is responsible for the up-regulated P_i transport observed with platelet-derived growth factor treatment of osteoblast-like cells. (*Kavanaugh and Kabat 1996; Kavanaugh et al. 1994; Kim and Cunningham 1993*). In osteoblasts it is possible that the more ubiquitously expressed type III Na/P_i transporters, such as Pit-1 and Pit-2, might be involved in the PKC-regulated uptake of P_i. Conversely, activation of PKC has been reported to inhibit P_i uptake in opossum kidney cells, which may indicate different regulation of the renal type I and II transporters (*Chien et al. 1998; Lehel et al 1995; Marsh and Helenius 1989*). These differences in PKC-mediated regulation of P_i uptake may be a consequence of different expression patterns of either PKC and/or Na/P_i transporter isotypes in different cell lines.

One of the major difficulties in determining which PKC isotypes are involved in regulating Na/P_i transport is that different cell types express various combinations of

PKC isoforms. Protein kinase C is a family of at least 11 serine- and threonine-specific phosphotransferase isoenzymes that are characterized by a high degree of homology in their catalytic and cysteine-rich domains. Although the possible role(s) of different PKC isozymes in cell growth and differentiation has been well studied (for review, see *Nishizuka and Nakamura 1995*), much less is known of their potential involvement in modulating intracellular trafficking of transmembrane receptors and up-regulation of ion transporters. In this study we have sought to determine which type of Na/P_i transporter/viral receptor is regulated by PMA activation of PKC and which PKC isotype(s) may be involved in the up-regulation of Na/P_i uptake in NIH 3T3 cells. The results presented in this thesis indicate that the Pit-2 Na/P_i transporter/viral receptor is specifically activated by PMA stimulation of PKC$^{\varepsilon}$.

Materials and Methods

Materials-- Dulbecco's modified Eagle's medium (DMEM) and fetal calf serum were purchased from Biofluids Inc. (Rockville, MD). PMA, bisindolylmaleimide, and Gö 6976 were products of Calbiochem (San Diego, CA). ^{32}P-Labeled monopotassium phosphate was from ICN (Costa Mesa, CA). The PKC isotype-specific antisense and scrambled oligonucleotides (ISIS 17260, PKC$^{\varepsilon}$ antisense; ISIS 17261, PKC$^{\varepsilon}$ scrambled control) were from ISIS Pharmaceuticals. PKC$^{\varepsilon}$ isotype-specific polyclonal antibodies were purchased from Life Technologies, Inc.; PKC$^{\alpha}$-specific monoclonal antibodies were from Upstate Biotechnology (Lake Placid, NY); and PKC$^{\delta}$- and PKC$^{\zeta}$-specific monoclonal antibodies were from Transduction Laboratories (Lexington, KY).

The pEGFP-N1 enhanced GFP (EGFP) tagging vector is available from Clontech (Palo Alto, Calif.), and the Xpress protein expression system (pTrcHis) and plasmids coding for endoplasmic reticulum (ER)- and mitochondrion-targeted GFP were obtained from Invitrogen (San Diego, Calif.). The early endosomal protein (EEA1) fragment (amino acids 1252 to 1411)-EGFP chimera was a gift from Tamás Balla (National Institute of Child Health and Human Development, National Institutes of Health, Bethesda, Md.). The p$^{\varepsilon}$MTH expression vector was developed in our laboratory as described previously (*Olah et al. 1994*). LysoTracker DND-99, Texas red-conjugated transferrin, Alexa 488 phalloidin, and dextran 10 were purchased from Molecular Probes, Inc. (Eugene, Oregon, USA).

Primary antibodies. PKC$^{\varepsilon}$ isotype-specific polyclonal antibodies (Gibco BRL, Gaithersburg, Maryland, USA) were used to detect $^{\varepsilon}$-epitope-tagged Pit-2 proteins. Anti-GFP polyclonal antibody was purchased from Chemicon International Inc. (Temecula, California, USA). The Pit-2-specific rabbit antiserum was produced in our laboratory using a recombinant HaPit-2 (the hamster homolog of Pit-2) cytoplasmic loop fragment (amino acids 272 to 462) as antigen (*Wilson et al. 1995*). The bacterial recombinant vector, pTrcHisA-EARcA21, expressing this fragment was overexpressed in *Escherichia coli* and then affinity purified using a His-Ni^{2+} column (Novagen, Madison, Wisconsin, USA). One and one-half milligrams of the approximately 95% pure cytosolic loop fragment protein was used as antigen for immunization of two rabbits. A-MuLV pig antiserum (lot no. 77S000445) and purified goat anti-Rausch

leukemia virus gp69/71 antibodies (lot no. 80S000018) were obtained from the NCI/BCB Reagents Repository (Camden, New Jersey, USA).

Secondary antibodies. Cy3-conjugated anti-rabbit and anti-mouse immunoglobulin (IgG), fluorescein-conjugated anti-pig IgG, and Texas red-conjugated anti-goat IgG secondary antibodies were purchased from Jackson ImmunoResearch Laboratories, Inc. (West Grove, Pennsylvania, USA). Peroxidase-labeled goat anti-rabbit and anti-mouse IgGs were from Kirkegaard & Perry Laboratories, Inc. (Gaithersburg, Maryland, USA.).

DNA constructs. (i) Primers. The PCR primers used were as follows:
1, GAGGTCGACATGGCCATGGATGAGTATTTGTGG;
2, *TCCTACTTTGGTGAAGAC*CTGATGCCCACAGGCAAATTACAAAAAGAAGGT GC; 3, *GTCTTCACCAAAGTAGGA*GAAGCCTTTTATTTTCCTCCGCATCCACGG;
4, GTATACGCGTCACATATGGAAGGATCCCATACATG;
5, GAAGCCCCGGGCCACATATGGAAGGATCCCATACATG. Recognition sites for restriction endonucleases used for cloning are underlined; overlapping sequences are italicized.

(ii) pTrcHisA-EARcA21. The *Sac*I-*Bam*HI restriction fragment of hamster Pit-2 (EAR, HaPit-2) was ligated into the pTrcHisA bacterial expression vector cut with *Sac*I-*Bgl*II.

(iii) pPit2$^{\varepsilon}$-$^{\varepsilon}$MTH. Insertion of the $^{\varepsilon}$-epitope tag into the cytoplasmic loop of Pit-2 was accomplished in two steps by overlapping PCR using primer pairs 1-2 and 3-4 in the first rounds of PCRs. The products of these reactions then were purified, annealed, and used as template for a final PCR using primers 1 and 4. The purified product was cut with *Sal*I-*Mlu*I and ligated into the p$^{\varepsilon}$MTH vector cut with *Xho*I-*Mlu*I. A second $^{\varepsilon}$-epitope tag was added at the C-terminal end of this cytosolic loop-tagged Pit-2$^{\varepsilon}$, with insertion and expression of this construct in the p$^{\varepsilon}$MTH vector.

(iv) pPit2-EGFPN1. Construction of human Pit-2 C-terminally tagged with GFP was accomplished using primers 1 and 5 to amplify human Pit-2 cDNA. The PCR-amplified product was cut with restriction endonucleases *Sal*I-*Xma*I and then ligated into the pEGFP-N1 vector.

Generation of overexpressor cell lines. -- The construction of expression vectors and establishment of PKC overproducer cell lines were carried out as described previously

(*Lehel et al. 1995*). The PKCa, -δ, -ε, and -ζ plasmid constructs were prepared in the pεMTH vector, and overexpressor cell lines were established following protocols described elsewhere (*Lehel et al 1994*). NIH 3T3 cells were transfected with either the control expression vector pεMTH or pPit2ε-εMTH, expressing the ε-epitope-tagged Pit-2, using electroporation. Stably transfected cell lines were selected with G418 (0.8 mg/ml). Individually picked colonies (10 from each transfection) were selected and pooled for further studies to minimize potential artifacts attributable to anomalies associated with special clones. The mixed populations of stable Pit-2εε overexpressor cells were used only through 12 to 14 passages in culture to negate possible outgrowth of one particular population of cells. NIH 3T3 and CHO-K1 cells also were transiently transfected by electroporation with either the control vector pEGFP-N1 or the pPit2-EGFPN1 expression vector. Cells transiently expressing Pit-2-GFP were used for further studies 24 h after transfection.

Cell Culture-- Retrovirus-infected and vector-transduced NIH 3T3 cells were cultured in DMEM supplemented with 10% fetal calf serum. After the cells reached confluency, the medium was changed to serum-free DMEM for 24 h. To induce overexpression of any ectopic gene products, the cells were incubated in the presence or absence of 20 μM zinc acetate, as indicated, to induce the up-regulation of the metallothionein promoter of the pεMTH vector (*Olah et al. 1994*).

Phosphate Uptake Measurement-- Sodium-dependent phosphate uptake was determined as described previously (*Olah et al 1993*).

Retrovirus Infections-- NIH 3T3 murine fibroblasts and mink lung fibroblasts (ATCC CCL 64) were maintained in DMEM supplemented with 10% (v/v) fetal bovine serum. NIH 3T3 cells were infected with wild type amphotropic murine retrovirus (A-MuLV) strain 4070A or the 57A Friend strain of ecotropic MuLV (E-MuLV). Mink fibroblasts expressing gibbon ape leukemia retrovirus (GALV)-competent PiT-1 were infected with wild type A-MuLV strain 4070A or infected with a GALV strain (SEATO), as described previously (*Olah et al. 1994*). Productive infection was monitored by measuring the reverse transcriptase activity found in the cell media of the infected cells (*Wilson and Eiden 1991*).

Cells productively infected with A-MuLV were demonstrated to be resistant to challenge infection with A-MuLV envelope vectors but not with E-MuLV envelope vectors. Cells productively infected with E-MuLV were resistant to E-MuLV envelope vectors but retained susceptibility to A-MuLV infectivity.

Antisense Oligonucleotide Treatment-- NIH 3T3 fibroblasts were cultured in 150-mm tissue culture dishes until they reached ~80% confluency. The cells then were harvested by trypsinization, washed with DMEM, and resuspended in 400 µl of cytosalt electroporation buffer (75% cytosalts (120 mM KCI, 0.15 mM $CaCl_2$, 10 mM K_2HP0_4, pH 7.6, 6.5 mM $MgCl_2$) and 25% Opti-MEM I). Twenty-µl aliquots of PKC isotype-specific or scrambled control oligonucleotides were added to the cells resuspended in prechilled BTX disposable electroporation cuvettes (P/N 640; 4-mm gap) to reach the indicated concentrations and then incubated on ice for 5 min. The oligonucleotides indicated were introduced into the cells by electroporation with a BTX Electro Square Porator (settings: low voltage mode, 99 msec; charge voltage, 475 V; pulse length, 1 msec; number of pulses, 4). The electroporated cells were kept at room temperature for 10 min and then seeded onto 100-mm tissue culture plates for immunoblot studies and onto 24-well plates for P_i uptake measurements. Western blot analysis of PKC isotypes and P_i uptake studies were carried out 24 h after introduction of the antisense oligonucleotides.

Western blot analysis. For protein extraction, cells were washed with ice-cold phosphate-buffered saline (PBS), harvested by scraping into lysis buffer (20 mM Tris-HCl [pH 7.4], 5 mM EGTA, 1 mM phenylmethylsulfonyl fluoride, 20 mM leupeptin), and disrupted in a Dounce homogenizer. Cell homogenates were fractionated by differential centrifugation into nuclear (pellet of $800 \times g$ centrifugation for 10 min), particulate (plasma membrane-enriched; $16,000 \times g$, 1-h pellet of the nucleus-free $800 \times g$ supernatant), and cytosolic ($16,000 \times g$ supernatant) fractions. Proteins of each fraction were separated by precast sodium dodecyl sulfate-4 to 20% polyacrylamide gel (Owl Separation Systems, Portsmouth, N.H.) electrophoresis and electrophoretically transferred from the gel onto Protran membranes (Schleicher & Schuell, Keene, N.H.); immunoreactive proteins were detected as described elsewhere (*Olah et al. 1994*).

Laser scanning confocal microscopy. NIH 3T3 cells were grown on glass multichamber slides. Vector control cells and cells overexpressing Pit-2$^{\varepsilon\varepsilon}$ (human Pit-2 protein double tagged with the $^{\varepsilon}$ epitope) were fixed in 4% buffered formaldehyde solution (Sigma) for 30 min at 4°C and then blocked with PBS containing 1% bovine serum albumin (BSA) and 0.6% Triton X-100 for 1 h at room temperature. Immunostaining was carried out with the indicated primary antibodies in the same PBS solution for 2 to 3 h at room temperature. After three 5-min washes in PBS, the appropriate secondary antibodies were applied for 1h at room temperature and washed with PBS. The slides then were mounted with Vectashield antifade reagent (Vector Laboratories, Burlingame, California) and covered with glass coverslips. Cells transiently overexpressing Pit-2-EGFP were labeled with cell organelle markers and mounted without fixation. For the LysoTracker, dextran 10, and transferrin receptor localization experiments, NIH 3T3 fibroblasts transiently transfected with pPit2-EGFPN1 by electroporation were plated on glass chamber slides and labeled with the markers 24 h posttransfection. Lysosomes were labeled with LysoTracker Red DND-99 according to the manufacturer's suggestions. To visualize the recycling endosome pool, cells were washed three times with serum-free DMEM and then incubated in the same medium containing 20 μg of Texas red-conjugated transferrin per ml for 30 min. The cells then were washed, chased with unlabeled transferrin (20 μg/ml) for 30 min, and mounted for fluorescence microscopy as described above. For labeling the late endosomal compartment, cells were incubated with 1 mg of Texas red-labeled dextran 10 per ml for 45 min, rinsed with medium, and incubated in fresh medium for 60 min to wash out the dextran prior to imaging. Confocal fluorescent images were collected with a Bio-Rad MRC 1024 confocal scan head mounted on a Nikon Optiphot microscope with a 40× or 60× planapochromat lens. A krypton-argon gas laser provided excitation at 488 and 568 nm. Emission filters of 598/40 and 522/32 were used for collecting red and green fluorescence, respectively, in channels 1 and 2, while phase-contrast images of the same cell were collected in the third channel using a transmitted light detector. After sequential excitation, red and green fluorescent images of the same cell were merged for colocalization of GFP with cellular organelle markers.

Results and Discussion

Most retroviruses have been found to use distinct cell surface receptors for specific cellular recognition and infection. Furthermore, studies have revealed that the normal cellular function of a number of these viral receptors is to serve as membrane transport proteins (*Weiss and Tailor 1995*). NIH 3T3 cells have been found to express several of these viral receptor/transporters, including Pit-1, Pit-2, and the cationic amino acid transporter CAT/y+, as determined by viral infection studies and reverse transcription-polymerase chain reaction analysis. NIH 3T3 cells are susceptible to infection by A-MuLV via Pit-2 and to infection with E-MuLV via the CAT/y+ amino acid transporter. However, because of the presence of specific point mutations in the endogenous murine Pit-1, Pit-1 is not functional as a GALV receptor in NIH 3T3 cells.

Effect of Viral Infection on PMA-induced Activation of Phosphate Transport-- Previous studies have established that infection of cells with retroviruses that selectively recognize either Pit-1 or Pit-2 resulted in the specific down-modulation of phosphate uptake mediated by that receptor/transporter (*Kavanaugh et al. 1994; Wilson et al. 1995*). A similar phenomenon has been observed to occur with the E-MuLV CAT/y+ receptor (*Wang et al. 1991; 1992*). To examine which of the viral receptor/P_i transporters are subject to regulation by PMA activation of PKC, studies were carried out with NIH 3T3 cells infected with different C-type retroviruses. The results presented in Fig. *1A* demonstrate that infection with A-MuLV decreased short term (2-min) basal Na/P_i transport (from 900 ± 91 to 404 ± 28 pmol of P_i/min/mg of protein) and, importantly, completely abolished the activation of P_i transport noted with exposure of cells to PMA. Infection of cells with E-MuLV would not be expected to alter P_i uptake, because this virus binds to a distinct cell surface cationic amino acid transporter (*Wang et al. 1991; 1992*). Thus, to control for possible pleiotropic effects of retrovirus infection on Na/P_i transport, P_i uptake experiments were carried out with NIH 3T3 cells infected with E-MuLV (Fig. *1B*). The results indicated that infection with E-MuLV did not alter either basal or PMA-induced Na/P_i transport.

As noted, GALV binds to the Pit-1 receptor of mink fibroblasts and selectively down-modulates P_i uptake caused by Pit-1 (*Olah et al. 1994*). To determine whether Na/P_i transport mediated by Pit-1 or Pit-2 is stimulated by activation of PKC, P_i uptake was measured in mink cells infected with either A-MuLV or GALV. Infection of these cells with A-MuLV again completely abolished the activation of P_i transport noted with exposure of cells to PMA (Fig. *1C*). Although GALV infection did result in an ~25% decrease in basal Na/P_i transport, which apparently is attributable to down-modulation of Pit-1, it did not decrease the PMA-induced stimulation of P_i uptake noted in these cells (Fig. *1D*). Taken together, these results obtained with C-type retrovirus-infected cells indicate that Pit-2 is the P_i transporter/viral receptor that is up-regulated with exposure of cells to PMA.

Effect of Selective PKC Inhibitors on PMA-induced Up-regulation of Pit-2 P_i Transport-- Although studies have established a general role for PKC in the regulation of several membrane transport mechanisms, little is known concerning the functional role(s) of specific PKC isotypes in these regulatory processes. Thus, studies were initiated to determine which PKC isotype(s) are involved in mediating the PMA-induced up-regulation of the Pit-2 transporter/receptor in NIH 3T3 cells. NIH 3T3 cells express a limited, but representative, set of different PKC isozymes (PKC^{α}, PKC^{δ}, PKC^{ε}, and PKC^{ζ}) (*Lehel et al. 1994; Mischak et al. 1993*). Because PMA does not directly activate atypical PKC^{ζ}, this isotype would not appear to be involved in the short term PMA-induced activation of Pit-2 P_i transport. Thus, experiments were initiated to address which class of PKC isoform stimulates P_i transport in response to activation by PMA. Two different PKC inhibitors were used to determine whether the PMA-induced activation of Na/P_i transport in NIH 3T3 cells was mediated via a conventional, Ca^{2+}-dependent (PKC^{α}), or a novel, Ca^{2+}-independent (PKC^{δ} and PKC^{ε}), isotype. Addition of the pan-specific bisindolylmaleimide inhibitor, which inhibits both classical and novel isotypes, resulted in pronounced inhibition of the PMA-induced activation of Na/P_i uptake (Fig. 2). Conversely, treatment of the cells with the Gö 6976 PKC inhibitor, which selectively inhibits only the classical PKC isotypes, did not cause significant inhibition of the PMA-induced up-regulation of P_i transport. These results

suggested that the classical PKC$^{\alpha}$ isoform likely was not involved in mediating the activation of Na/P_i uptake by Pit-2 with exposure of NIH 3T3 cells to PMA.

Effect of Overexpression of PKC Isotypes on Na/P_i Uptake-- To further resolve which of the PKC isotype(s) may be involved in mediating the PMA activation of the Na/P_i uptake, we used NIH 3T3 cells overexpressing PKC$^{\alpha}$, -$^{\delta}$, -$^{\varepsilon}$, or -$^{\zeta}$ isozymes to determine the ability of each isotype to enhance Pit-2 P_i transport activity in the absence of PMA treatment. The cell cultures were shifted to serum-free media and incubated in the presence of 20 μM zinc acetate for 24 h to enhance expression of the indicated PKC isotype directed by the metallothionein promoter of the p$^{\varepsilon}$-MTH vector. Overexpression of PKC$^{\varepsilon}$ was found to increase Na/P_i uptake, whereas overexpression of PKC$^{\alpha}$, PKC$^{\delta}$, and PKC$^{\zeta}$ did not appreciably alter the level of P_i transport relative to the level determined in vector control cells (Fig. 3A). Exposure of the PKC$^{\varepsilon}$ overexpressor cells to 1 μM PMA resulted in only an additional 15-20% increase in P_i transport. Western blot analysis showed that the level of expression was similar for each of the $^{\varepsilon}$ epitope-tagged PKC isotypes (Fig. 3B). These results indicate that the selective overexpression of PKC$^{\varepsilon}$ alone can mimic the stimulation of Na/P_i uptake observed with PMA treatment of wild type cells.

Effect of PKC$^{\varepsilon}$-specific Antisense Oligonucleotide on PMA-induced Stimulation of Pit-2 P_i Transport-- To further support the findings that PKC$^{\varepsilon}$ is the isotype involved in mediating the PMA-induced activation of the Pit-2 P_i transporter, studies were carried out with PKC$^{\varepsilon}$-selective antisense oligonucleotide (AON) to specifically inhibit PKC-$^{\varepsilon}$ in the cell. As shown in Fig. 4A, pretreatment of NIH 3T3 cells with increasing concentrations of PKC$^{\varepsilon}$-AON significantly decreased the expressed levels of PKC$^{\varepsilon}$ and had no effect on the levels of PKC$^{\alpha}$, PKC$^{\delta}$, or PKC$^{\zeta}$. Densitometric scanning to quantitate the intensity of the PKC$^{\varepsilon}$ bands of cells treated with PKC$^{\varepsilon}$-AON relative to AON scrambled controls indicated relative band densities of 1.0, 0.59, and 0.28 with 0.24, 1.2, and 2.4 mM oligonucleotide treatment, respectively. Importantly, treatment of the cells with PKC$^{\varepsilon}$-AON did result in inhibition of PMA-induced up-regulation of P_i transport (Fig. 4B). Treatment of cells with scrambled oligonucleotides did not have any effect on either the intracellular level of PKC$^{\varepsilon}$ or PMA activation of Na/P_i uptake.

Similar experiments with PKC$^{\delta}$-AON (ISIS 17254) caused a significant decrease in the levels of PKC$^{\delta}$ but had no effect on PMA-induced stimulation of P_i uptake (data not shown). These data provide additional evidence to support the exclusive involvement of PKC$^{\varepsilon}$ in mediating PMA activation of Pit-2.

The suggestion that different PKC isotypes play distinct functional roles in the cell by phosphorylating either isoform- or subcellular compartment-specific substrates is widely accepted. However, few studies have been reported that establish that a specific PKC isotype may selectively regulate a given biological function. Although a role for PKC has been implicated in the regulation of numerous membrane transport mechanisms (*Veldman et al. 1998; Ribeiro et al. 1996; Corey et al 1994; Enyedi et al. 1996; Rokaw et al 1996*), little information is available on the specific PKC isotype(s) involved in the regulation of these transport activities. Karim et al. attributed the modulation of the Na/H antiport to both PKC$^{\alpha}$ and PKC$^{\varepsilon}$. PKC$^{\varepsilon}$ also has been implicated in the stimulation of anionic amino acid transport (*Franchi-Gazzola et al. 1996*), and treatment with antisense oligonucleotides to PKC$^{\delta}$ has been shown to block the $^{\alpha}$1-adrenergic activation of Na-K-2Cl cotransport (*Liedtke and Cole 1997*). The evidence reported here indicates that PKC$^{\varepsilon}$ is involved in mediating the PMA-induced up-regulation of Na/P_i uptake by the Pit-2 transporter/viral receptor.

The Pit-1 and Pit-2 viral receptor/P_i transporters share 56% amino acid identity (*van Zeijl et al. 1994*). Hydropathy analysis of Pit-1 and Pit-2 suggested the presence of at least two clusters of putative transmembrane-spanning sequences, along with a large intracellular hydrophilic domain located between the sixth and seventh transmembrane helices (*Olah et al 1994; Wilson and Eiden 1991*). There are a number of consensus phosphorylation sites in both Pit-1 and Pit-2, particularly within the hydrophilic loop domain. Thus, it is likely that PKC$^{\varepsilon}$ may directly phosphorylate Pit-2 to stimulate Na/P_i uptake.

However, another mechanism of regulation found with other transporters is induced redistribution of the transporter from intracellular stores to the plasma membrane. For example, insulin has been reported to regulate the intracellular trafficking of glucose transporter 4 (*Hudson et al. 1992*). Previously, we have shown that PKC$^{\varepsilon}$ can regulate

Golgi-related functions, including protein trafficking and secretion (*Lehel et al. 1995*). To address this possibility, studies were carried out to determine whether PMA still was able to enhance P_i uptake under conditions in which vesicle trafficking from the Golgi to the plasma membrane was blocked by incubating cells at room temperature and by treatment of cells with nocodazole (to disrupt microtubules) and cytochalasin D (to disrupt actin filaments). It was found that these treatments did not block PMA-induced activation of P_i uptake.[2] Although these results indicate that PKCε does not act by modulating the trafficking of PiT-2 from the Golgi to the plasma membrane, they do not fully rule out the possibility that PKCε might act to mediate the rapid recruitment (fusion) of an existing pool of Pit-2-containing vesicles to the plasma membrane.

In addition to their role as representative members of an important family of phosphate transporters, Pit-1 and Pit-2 are of particular interest as the cell surface receptors for the GALV and A-MuLV retroviruses, respectively. Many current gene therapy protocols use GALV- or A-MuLV-enveloped vectors (*Barquinero et al 1995; Kavanaugh and Kabat 1996*). A basic knowledge of murine leukemia virus receptor regulation and trafficking is likely to be useful in the development and improvement of gene therapy protocols based on the use of these retroviral vectors. Although our results clearly indicate that PKCε is involved in regulating Na/P_i uptake by Pit-2, it remains to be determined whether PKCε-mediated regulation of the Pit-2 transporter/viral receptor might influence recognition of the viral envelope protein and viral entry into the cell.

ε-Epitope-tagged human Pit-2 overexpressed in NIH 3T3 fibroblasts and GFP-tagged human Pit-2 overexpressed in CHO-K1 cells retain their functional and regulatory properties. PCR products of Pit-2 were produced and then cloned into either the pεMTH or pEGFP-N1 vector as described in Materials and Methods. The resulting Pit2ε–εMTH construct (Fig. 5A) was used to transfect NIH 3T3 cells, and cell lines stably overexpressing Pit-2εε were selected. Overexpression of Pit-2εε in NIH 3T3 fibroblasts resulted in only a slight increase in P_i uptake. However, following Zn^{2+} induction of the metallothionein promoter to enhance expression of the Pit-2εε protein, P_i uptake was significantly increased (160%) compared to vector control. Moreover, ε-

epitope-tagged Pit-2 transporters retained the ability to be up-regulated by PMA, as demonstrated by a proportional increase in P_i uptake detected with the tagged Pit-2 transporters following PMA treatment of the overexpressor cells (Fig. 5C). A-MuLV infection of the Pit-2εε overexpressor cells resulted in a significant (60%) decrease in P_i uptake activity, indicating that the P_i transporter activity of the tagged Pit-2 molecules was blocked by A-MuLV infection in a manner similar to that observed with the native or wild-type Pit-2 transporters (Fig. 5D). CHO-K1 cells normally are resistant to A-MuLV infection due to the presence of inhibitors secreted by CHO-K1 cells that can inhibit endogenous HaPit-2 receptor function. This resistance can be overcome by expressing the human form of the Pit-2 transporters/receptors in CHO-K1 cells. To test the Pit-2–EGFP chimera (Fig. 5B) for A-MuLV receptor function, we transiently transfected plasmid pPit2-EGFP into CHO-K1 cells and then infected the transiently transfected cells with A-MuLV vectors carrying a ß-galactosidase reporter gene as described elsewhere ((*Chaudry et al. 1999*). CHO-K1 cells transfected with pPit2-EGFP were found to be sensitive to A-MuLV, as indicated by the formation of blue foci in response to expression of the ß-galactosidase reporter gene. No blue foci were detected in CHO-K1 cells transfected with the control pEGFP-N1 and A-MuLV vectors (data not shown). As expected, since CHO-K1 cells are resistant to A-MuLV infection, the virus titer obtained for A-MuLV vectors on CHO-K1 control was 0 infectious unit/ml. The titer obtained with CHO-K1 cells expressing Pit-2 was 2,000 infectious units/ml, which compared to a value of 1,800 infectious units/ml with CHO-K1 cells expressing epitope-tagged Pit-2. Further, expression of the Pit-2–EGFP chimera significantly increased P_i uptake compared to vector control, and PMA treatment enhanced Pit-2–EGFP-mediated P_i transport (data not shown). These results indicate that the ε-epitope-tagged Pit-2 and the Pit-2–EGFP chimera both retain A-MuLV receptor function and that both Pit-2εε and Pit-2–EGFP retain all of the functional and regulatory characteristics of wild-type Pit-2 phosphate transporter activity.

Western blot analysis of overexpressed ε-epitope- and GFP-tagged human Pit-2 phosphate transporter/retrovirus receptor proteins in NIH 3T3 cell lysates. Immunostaining of protein blots of a plasma membrane enriched particulate fraction

prepared from Pit-2εε overexpressor cells with anti-ε antibody revealed an immunoreactive 70-kDa band (Fig. 6A, lane 2). Interestingly, the ε-epitope-tagged Pit-2 protein detected in the 16,000 × *g* particulate fraction prepared from A-MuLV-infected cells was found to migrate as a lower-molecular-mass protein of about 60 kDa (Fig. 6A, lane 3). The change in Pit-2 receptor migration rate was specific for A-MuLV-infected cells. Pit-2 detected in the particulate fraction prepared from cells infected with ecotropic Moloney MuLV (which binds to the cationic amino acid transporter, M-CAT1), migrated at a molecular weight similar to that observed with the uninfected control cells (Fig. 6A, lane 4). No immunoreactive Pit-2εε band was detected in the protein sample prepared from the vector control cell line (Fig. 6A, lane 1). Endogenous PKCε was detected with the anti-PKCε antibody as a 90-kDa band and served as an internal control of the amount of protein loaded per lane. Western blot analysis using anti-HaPit-2 rabbit antiserum in place of the ε-tag antibody resulted in a similar pattern (Fig. 6B). Again, Pit-2 was found to migrate as a lower-molecular-weight band in A-MuLV-infected NIH 3T3 cells compared to uninfected and ecotropic Moloney MuLV-infected cells. These results indicate that infection of NIH 3T3 cells expressing epitope-tagged Pit-2 with A-MuLV (which utilizes Pit-2 as its cell surface receptor) correlates with the presence of a more rapidly migrating form of Pit-2 and results in the loss of P$_i$ transporter function. One explanation for this observation is that the Pit-2 present in A-MuLV-infected cells is more susceptible to a peptidase, which may catalyze the proteolytic processing of Pit-2. A second possibility is that the band shift noted with Pit-2 concomitant with A-MuLV superinfection may be due to the blockage of required posttranslational modifications such as phosphorylation and/or glycosylation which may take place before or at the time of Pit-2 trafficking to the plasma membrane. In a related study using Moloney MuLV-infected NIH 3T3 cells, the MCAT-1 ecotropic virus receptor was observed to also migrate as a lower-molecular-weight protein. This increase in electrophoretic mobility noted with MCAT-1 from infected cells was found to be due to a blockage of normal N-linked glycosylation. It was proposed that binding of newly synthesized ecotropic virus envelope surface protein, gp70, with the MCAT-1 receptor in the ER acted to prevent normal glycosylation of MCAT-1 (*Kim and Cunningham 1993*).

Subcellular redistribution of Pit-2εε in NIH 3T3 cells productively infected with A-MuLV. Fluorescence laser confocal microscopy was used to provide optical sectioning of cells. Basically, the image obtained with confocal laser microscopy is equivalent to a thin section across the entire length or width of the cell and does not represent the cell as a whole. The results obtained revealed that Pit-2εε localized mainly to the plasma membrane when overexpressed in control NIH 3T3 cells (Fig. 7A, 1 and 2; Fig. 7B, 2 control). In addition, faint staining also was detected at a perinuclear location in some of those uninfected cells. This may represent a Golgi-localized pool of newly synthesized Pit-2εε. Likewise, Pit-2–GFP transiently coexpressed in the Pit-2εε overexpressor cells also exhibited plasma membrane localization (Fig. 7B, 1 control). Importantly, the epitope-tagged Pit-2 was not detected at the plasma membrane following productive infection of the overexpressor cells with A-MuLV; rather, it was found predominantly redistributed to an unidentified intracellular location (Fig. 7A, 3; Fig. 7B, 2 A-MuLV). Some staining was detected at an apparent nuclear membrane location in A-MuLV-infected cells. A similar pattern of Pit-2–GFP redistribution was observed when A-MuLV producer Pit-2εε overexpressor cells were transiently transfected with the pPit2-EGFPN1 construct (Fig. 7B, 1 A-MuLV). Merging of Fig. 3B pictures 1 and 2 resulted in areas of yellow signal indicating colocalization of Pit-2εε and Pit-2–GFP (Fig. 7B, 3). In both infected and uninfected NIH 3T3 fibroblasts, the ε-epitope-tagged Pit-2 transporters colocalized with the Pit-2–GFP chimeras, indicating that the presence of the bulky GFP protein at the C terminus did not affect the localization of Pit-2–GFP (Fig. 7B, 3). The epitope-tagged Pit-2 transporters remained localized to the plasma membrane in ecotropic Moloney MuLV (Fig. 7A, 4)- and 57A Friend MuLV (not shown)-producing cells, indicating that the observed redistribution of Pit-2 was A-MuLV specific and not attributable to general effects associated with retroviral infection.

Colocalization of A-MuLV envelope protein with the overexpressed epitope-tagged Pit2 transporter/receptor in productively infected Pit-2 overexpressor NIH 3T3 cells. To define the relationship between infection of cells with A-MuLV and the redistribution of Pit-2 receptor within the virus producer fibroblasts, double

immunostaining experiments were performed with fluorescent labeling and confocal microscopy using A-MuLV-specific pig antiserum and antibodies against the ε-epitope tag of Pit-2εε as described in Materials and Methods. Anti-ε-epitope staining for Pit-2εε in the A-MuLV-infected cells using Cy3-conjugated secondary antibodies resulted in the characteristic punctate intracellular (internalized) pattern noted previously for Pit-2εε in productively infected cells (Fig. 7C, Pit-2εε). The distribution of A-MuLV within the infected NIH 3T3 cells was visualized by fluorescein-conjugated goat anti-pig IgG secondary antibodies. Uninfected cells were stained in the same way to set the background signal to zero. A-MuLV particles also appeared as disperse punctate structures throughout the cytoplasm, with denser distribution occurring in areas similar to the patterns represented by Pit-2εε (Fig. 3C, A-MuLV). Merging of the pictures resulted in areas of yellow signal indicating colocalization of Pit-2 and A-MuLV in punctate structures throughout the cytosol (Fig. 7C, merged). Alternatively, A-MuLV-infected NIH 3T3 cells were transiently transfected with the pPit2-EGFPN1 construct and stained for A-MuLV gp70 envelope protein with goat anti-Rausch murine leukemia virus gp69/71 antibody using Texas red-conjugated anti-goat IgG secondary antibodies. This goat anti-Rausch murine leukemia virus gp69/71 antibody has been shown to recognize the proline-rich region of MuLV protein, including the A-MuLV gp70 envelope protein (*Weimin Wu et al. 1998*). The distribution of Pit-2–GFP and A-MuLV gp70 protein was visualized under laser scanning confocal microscopy as described in Materials and Methods. Again, Pit-2–GFP showed subcellular localization similar to A-MuLV gp70, and merging the pictures resulted in yellow areas indicating colocalization of Pit-2–GFP and A-MuLV gp70 envelope protein (Fig. 7D).

Pit-2εε overexpressed in A-MuLV producer fibroblasts did not colocalize with commonly used markers for intracellular organelles. The pattern of subcellular redistribution of Pit-2εε in A-MuLV-infected cells was similar in some respect to that reported for the human immunodeficiency virus type 1-induced redistribution of CD4 molecules to the ER (*Bour et al. 1995*). Therefore, we used ER-targeted GFP to determine a possible colocalization with Pit-2εε in A-MuLV-infected fibroblasts.

Double-channel fluorescent laser confocal imaging of Pit-2εε-overexpressing A-MuLV producer cells showed no colocalization of Pit-2εε with the ER marker GFP (Fig. 8C). Furthermore, no colocalization of Pit-2εε was observed either with GFP alone (which exhibits both cytoplasmic and nuclear staining) (Fig. 8A) or with a PKCε zinc finger fragment 3-GFP chimera (which localizes predominantly to the Golgi complex (Lehel et al. 1995) (Fig. 8B). To test the possibility that a modified Pit-2 may be redistributed to the lysosomes rather than transported to the plasma membrane, we assessed the subcellular localization of Pit-2–GFP chimeras in live cells stained with the lysosome marker LysoTracker as described in Materials and Methods. Again, no colocalization of Pit-2–GFP with the lysosome marker was observed in the A-MuLV-infected cells (Fig. 8G). Experiments using Texas red-conjugated transferrin (a marker for recycling endosomes) or dextran 10 (a marker for late endosomes) together with Pit-2–GFP showed no colocalization with Pit-2–GFP in A-MuLV-infected live fibroblasts (Fig. 8E and F). Moreover, the subcellular localization of the epitope-tagged Pit-2εε pool was found to be different from that for mitochondria (with mitochondrion-targeted GFP as a marker) (data not shown) and from that for early endosomes with EEA1-GFP chimeras as a marker (Fig. 8D).

Recently, it was reported that Pit-2 formed a physical association with actin (*Rodrigues and Heard 1999*). Further, the formation of actin stress fibers was implicated in determining the cell surface distribution of Pit-2, the internalization of the receptor in response to virus binding, and the capacity to process retrovirus entry. To determine whether the reported association between Pit-2 and actin was conserved after A-MuLV infection, A-MuLV producer Pit-2εε-overexpressing cells were double stained with ε-tag antibody to detect Pit-2εε- and fluorescein-conjugated phalloidin to detect actin stress fibers. We were unable to detect colocalization of Pit-2εε and the actin network within A-MuLV producer fibroblasts (Fig. 8H). In addition, no apparent loss of actin cytoskeletal integrity was detected under those conditions, which might result from the loss of actin stress fibers or aggregation of actin near the cell surface as described for other oncoretroviral transformation (*Burridge 1985*).

Cells infected with one retrovirus are typically resistant to superinfection with the same virus or other viruses that utilize the same receptor. This phenomenon of superinfection interference often involves the down-modulation of a specific cell surface viral receptor. For several retroviruses, interference involves depletion of receptors from the surface of infected cells. However, other mechanisms for superinfection interference have been proposed. For example, E-MuLV has been reported to bind to a conformationally mobile site on the mouse MCAT-1 receptor (*Wang et al 1992*). Binding of the envelope glycoprotein gp70 to the MCAT-1 viral receptor/basic amino acid transporter appears to slow down a conformational transition of the empty transporter required to move the viral binding site from the inside back to the outside of the cell. This results in a significant decrease in further viral infection mediated through this receptor. Yet the infected cells retain basic amino acid transport activity, which is required for cell viability. It has been suggested that interference in response to human immunodeficiency virus type 1 infection is more complex than with simpler retroviruses such as A-MuLV. In addition to *env*, at least two other genes also have been reported to contribute to this process. The product of *vpu* interacts with newly synthesized CD4 and causes its degradation if it is associated with the envelope protein, while *nef* expression causes loss of the CD4 receptor from the cell surface (*Bour et al. 1995*). Infection by cytopathic retroviruses such as certain strains of feline leukemia virus is not associated with superinfection interference. It has been suggested that this delay or failure to establish superinfection interference may be responsible for the cell killing noted with infection by such cytopathic viruses (*Temin 1986*). However, infection with other subgroups of FeLV does lead to superinfection interference. This FeLV subgroup-specific superinfection interference does not appear to be due to a blockade or down-regulation of other cell components required for virus entry (*Reinhart et al. 1993*).

Infection of cells with A-MuLV does induce resistance to superinfection, and it has been proposed that this interference may in part involve down-modulation of the Pit-2 receptor (*Kavanaugh and Kabat 1996*). Previously, it was established that Pit-2-mediated Na^+/P_i uptake can be specifically blocked by infection of cells with A-MuLV (*Wilson et al 1995*), and expression of the amphotropic envelope protein in murine cells also was shown to inhibit phosphate transport mediated by Pit-2 (*Kavanaugh et al*

1994). However, the mechanism responsible for the loss of Pit-2 transporter and viral receptor functions with A-MuLV infection has not yet been elucidated. Here we have presented experimental findings obtained with epitope-tagged forms of human Pit-2 designed to determine the fate of Pit-2 in A-MuLV-infected cells. Results are presented to show that the tagged Pit-2 receptors are localized to the plasma membrane in uninfected NIH 3T3 cells. However, when cells expressing the tagged Pit-2 were productively infected with A-MuLV, the tagged protein was no longer present at the plasma membrane. Rather, tagged Pit-2 now was found distributed to punctate structures within the cytosolic compartment, where it was found to colocalize with the A-MuLV gp70 envelope protein. The intracellular pool of epitope-tagged Pit-2 phosphate transporter/viral receptor present in A-MuLV-infected cells was shown to be a more rapidly migrating, apparently lower-molecular-weight form of Pit-2. A-MuLV, but not E-MuLV, appears to infect cells by releasing nucleocapsid into the cytoplasm following direct fusion at the plasma membrane and not through an endocytic pathway as a complex with Pit-2 receptor (*Marsh and Helenius 1989*). Thus, the loss of Pit-2 from the plasma membrane in A-MuLV-infected cells does not appear to be due to a virus-induced endocytic process. Rather, it is conceivable that in A-MuLV-infected cells, complexes of newly synthesized Pit-2 receptor and the A-MuLV envelope glycoprotein may form shortly after protein synthesis. The newly synthesized Pit-2 found in these complexes may not be available for required covalent modifications or may be more susceptible to proteolytic modification. In turn, the posttranslational modifications blocked with the formation of intracellular Pit-2-A-MuLV envelope protein complexes may be required for normal Pit-2 processing and trafficking to the plasma membrane. The absence of Pit-2 receptors from the plasma membrane appears to be responsible for the superinfection interference observed in cells productively infected with A-MuLV.

Summary

The membrane receptors for the gibbon ape leukemia retrovirus and the amphotropic murine retrovirus serve normal cellular functions as sodium-dependent phosphate transporters (Pit-1 and Pit-2, respectively). Earlier studies established that activation of protein kinase C (PKC) by treatment of cells with phorbol 12-myristate 13-acetate (PMA) enhanced sodium-dependent phosphate (Na/Pi) uptake. Studies now have been carried out to determine which type of Na/Pi transporter (Pit-1 or Pit-2) is regulated by PKC and which PKC isotypes are involved in the up-regulation of Na/Pi uptake by the Na/Pi transporter/viral receptor. It was found that the activation of short term (2-min) Na/Pi uptake by PMA is abolished when cells are infected with amphotropic murine retrovirus (binds Pit-2 receptor) but not with gibbon ape leukemia retrovirus (binds Pit-1 receptor), indicating that Pit-2 is the form of Na/Pi transporter/viral receptor regulated by PKC. The PKC-mediated activation of Pit-2 was blocked by pretreating cells with the pan-PKC inhibitor bisindolylmaleimide but not with the conventional PKC isotype inhibitor Go 6976, suggesting that a novel PKC isotype is required to regulate Pit-2. Overexpression of PKCepsilon, but not of PKCalpha, -delta, or -zeta, was found to mimic the activation of Na/Pi uptake. To further establish that PKCepsilon is involved in the regulation of Pit-2, cells were treated with PKCepsilon-selective antisense oligonucleotides. Treatment with PKCepsilon antisense oligonucleotides decreased the PMA-induced activation of Na/Pi uptake. These results indicate that PMA-induced stimulation of Na/Pi uptake by Pit-2 is specifically mediated through activation of PKCepsilon.

Amphotropic murine leukemia virus (A-MuLV) utilizes the Pit-2 sodium-dependent phosphate transporter as a cell surface receptor to infect mammalian cells. Previous studies established that infection of cells with A-MuLV resulted in the specific down-modulation of phosphate uptake mediated by Pit-2 and in resistance to superinfection with A-MuLV. To study the mechanisms underlying these phenomena, we constructed plasmids capable of efficiently expressing epsilon epitope- and green fluorescent protein (GFP)-tagged human Pit-2 proteins in mammalian cells. Overexpression of epsilon-epitope-tagged Pit-2 transporters in NIH 3T3 cells resulted in a marked increase

in sodium-dependent P(i) uptake. This increase in P(i) uptake was specifically blocked by A-MuLV infection but not by infection with ecotropic MuLV (E-MuLV) (which utilizes a cationic amino acid transporter, not Pit-2, as a cell surface receptor). These data, together with the finding that the tagged Pit-2 transporters retained their A-MuLV receptor function, indicate that the insertion of epitope tags does not affect either retrovirus receptor or P(i) transporter function. The overexpressed epitope-tagged transporters were detected in cell lysates, by Western blot analysis using both epsilon-epitope- and GFP-specific antibodies as well as with Pit-2 antiserum. Both the epitope- and GFP-tagged transporters showed almost exclusive plasma membrane localization when expressed in NIH 3T3 cells, as determined by laser scanning confocal microscopy. Importantly, when NIH 3T3 cells expressing these proteins were productively infected with A-MuLV, the tagged transporters and receptors were no longer detected in the plasma membrane but rather were localized to a punctate structure within the cytosolic compartment distinct from Golgi, endoplasmic reticulum, endosomes, lysosomes, and mitochondria. The intracellular Pit-2 pool colocalized with the virus in A-MuLV-infected cells. A similar redistribution of the tagged Pit-2 proteins was not observed following infection with E-MuLV, indicating that the redistribution of Pit-2 is not directly attributable to general effects associated with retroviral infection but rather is a specific consequence of A-MuLV-Pit-2 interactions.

References

Arao, M., Yamaguchi, T., Sugimoto, T., Fukase, M., and Chihara, K. 1994 Eur. J. Endocrinol. **131**, 646-651

Barquinero, J., Kiem, H. P., von Kalle, C., Darovsky, B., Goehle, S., Graham, T., Seidel, K., Storb, R., and Schuening, F. G. 1995 Blood **85**, 1195-1201

Batra, R. K., J. C Olsen, R. J. Pickles, D. K. Hoganson, and R. C. Boucher. 1998. Am. J. Respir. Cell Mol. Biol. **18:**402-410

Bour, S., R. Geleziunas, and M. A. Wainberg. 1995. Microbiol. Rev. **59:**63-93

Burridge, K. 1986. Cancer Rev. **4:**18-78.

Cardinali, M., J. Jakus, S. Shah, J. F. Ensley, K. C. Robbins, and W. A. Yeudall. 1998. Oral Oncol. **34:**211-218

Caverzasio, J., and Bonjour, J. P. 1996 Kidney. Int. **49**, 975-980

Chaudry, G. J., K. B. Farrell, Y.-T. Ting, C. Schmitz, Y. S. Lie, C. J. Petropoulos, and M. V. Eiden.1999. J. Virol. **73:**2916-2920

Chien, M. L., E. O'Neill, and J. V. Garcia. 1998. Virology **240:**109-117

Coffin, J. M. 1996. Retroviridae, p. 1767-1848. *In* D. M. Knipe, P. M. Howley, and B. N. Fields (ed.), Field's virology, vol. 2. Lippincott, Philadelphia, Pa.

Eglitis, M. A., M. V. Eiden, and C. A. Wilson.1993. J. Virol. **67:**5472-5477

Corey, J. L., Davidson, N., Lester, H. A., Brecha, N., and Quick, M. W. 1994 J. Biol. Chem. **269**, 14759-14767

Eiden, M. V., K. B. Farrell, and C. A. Wilson.1996. J. Virol. **70:**1080-1085

Enyedi, A., Verma, A. K., Filoteo, A. G., and Penniston, J. T. 1996 J. Biol. Chem. **271**, 32461-32467

Franchi-Gazzola, R., Visigalli, R., Bussolati, O., and Gazzola, G. C. 1996 J. Biol. Chem. **271**, 26124-26130

Hudson, A. W., Ruiz, M., and Birnbaum, M. J.1992 J. Cell Biol. **116**, 785-797

Karim, Z., Defontaine, N., Paillard, M., and Poggioli, J 1995 Am. J. Physiol. **269**, C134-C140

Kavanaugh, M. P., and D. Kabat. 1996. Kidney Int. **49:**959-963

Kavanaugh, M. P., D. G. Miller, W. Zhang, W. Law, S. L. Kozak, D. Kabat, and A. D. Miller.1994. Proc. Natl. Acad. Sci. USA **91:**7071-7075

Kim, J. W., and J. M. Cunningham. 1993J. Biol. Chem. **268:**16316-16320

Lehel, C., Z. Olah, G. Jakab, and W. B. Anderson. 1995. Proc. Natl. Acad. Sci. USA **92:**1406-1410

Lehel, C, Olah, Z., Mischak, H., Mushinski, J. F., and Anderson, W. B. (1994) J. Biol. Chem. **269**, 4761-4766

Liedtke, C. M., and Cole, T. (1997) Am. J. Physiol. **273**, C1632-C1640

Marsh, M., and **A. Helenius.** 1989. Adv. Virus Res. **36:**107-151

Miller, A. D., and G. Wolgamot. 1997 J. Virol. **71:**4531-4535

Miller, D. G., R. H. Edwards, and A. D. Miller. 1994. Proc. Natl. Acad. Sci. USA **91:**78-82

Mischak, H., Goodnight, J., Kolch, W., Martiny-Baron, G., Schaechtle, C., Kazanietz, M. G., Blumberg, P. M., Pierce, J. H., and Mushinski, J. F. 1993 J. Biol. Chem. **268**, 6090-6096

Murer, H., Werner, A., Reshkin, S., Wuarin, F., and Biber, J. 1991 Am. J. Physiol. **260**, C885-C899

Nishizuka, Y., and Nakamura, S. 1995 Clin. Exp. Pharmacol. Physiol. **22 Suppl. 1**, S202-S203

Olah, Z., C. Lehel, and W. B. Anderson.1993. Biochim. Biophys. Acta **1176:**333-338

Olah, Z., C. Lehel, W. B. Anderson, M. V. Eiden, and C. A. Wilson. 1994. J. Biol. Chem. **269:**25426-25431

Olah, Z., C. Lehel, G. Jakab, and W. B. Anderson.1994. Anal. Biochem. **221:**94-102

Palmer, G., Bonjour, J. P., and Caverzasio, J. 1997 Endocrinology **138**, 5202-5209

Quamme, G., Biber, J., and Murer, H. 1989 Am. J. Physiol. **257**, F967-F973

Quamme, G., Pelech, S., Biber, J., and Murer, H. 1994 Biochim. Biophys. Acta **1223**, 107-116

Reinhart, T. A., A. K. Ghosh, E. A. Hoover, and J. I. Mullins 1993. J. Virol. **67:**5153-5162

Ribeiro, C. M. P., and Putney, J. W., Jr. 1996 J. Biol. Chem. **271**, 21522-21528

Rodrigues, P., and J. M. Heard. 1999. J. Virol. **73:**3789-3799

Schmid, C., Keller, C., Schlapfer, I., Veldman, C., and Zapf, J. 1998 Biochem. Biophys. Res. Commun. **245**, 220-225

Rokaw, M. D., West, M., and Johnson, J. P. 1996 J. Biol. Chem. **271**, 32468-32473

Temin, H. M. 1986. Rev. Infect. Dis. **10**:399-405.

van Zeijl, M., S. V. Johann, E. Closs, J. Cunningham, R. Eddy, T. B. Shows, and B. O'Hara. 1994.. Proc. Natl. Acad. Sci. USA **91**:1168-1172

Veldman, C. M., Schlapfer, I., and Schmid, C. 1997 Bone **21**, 41-47

Veldman, C. M., Schlapfer, I., and Schmid, C. 1998 Endocrinology **139**, 89-94

Wang, H., E. Dechant, M. Kavanaugh, R. A. North, and D. Kabat. 1992. J. Biol. Chem. **267**:23617-23624

Weimin Wu, B., P. M. Cannon, E. M. Gordon, F. L. Hall, and W. F. Anderson. 1998. J. Virol. **72**:5383-5391

Weiss, R. A., and Tailor, C. S. 1995 Cell **82**, 531-533

Wilson, C. A., and M. V. Eiden. 1991. J. Virol. **65**:5975-5982

Wilson, C. A., M. V. Eiden, W. B. Anderson, C. Lehel, and Z. Olah. 1995. J. Virol. **69**:534-537

Wilson, C. A., K. B. Farrell, and M. V. Eiden. 1994. J. Virol. **68**:7697-7703.

Yang, S., R. Delgado, S. R. King, C. Woffendin, C. S. Barker, Z. Y. Yang, L. Xu, G. P. Nolan, and G. J. Nabel. 1999.. Hum. Gene Ther. **10**:123-132

Zhen, X., Bonjour, J. P., and Caverzasio, J. 1997 J. Bone Miner. Res. **12**, 36-44

Figures

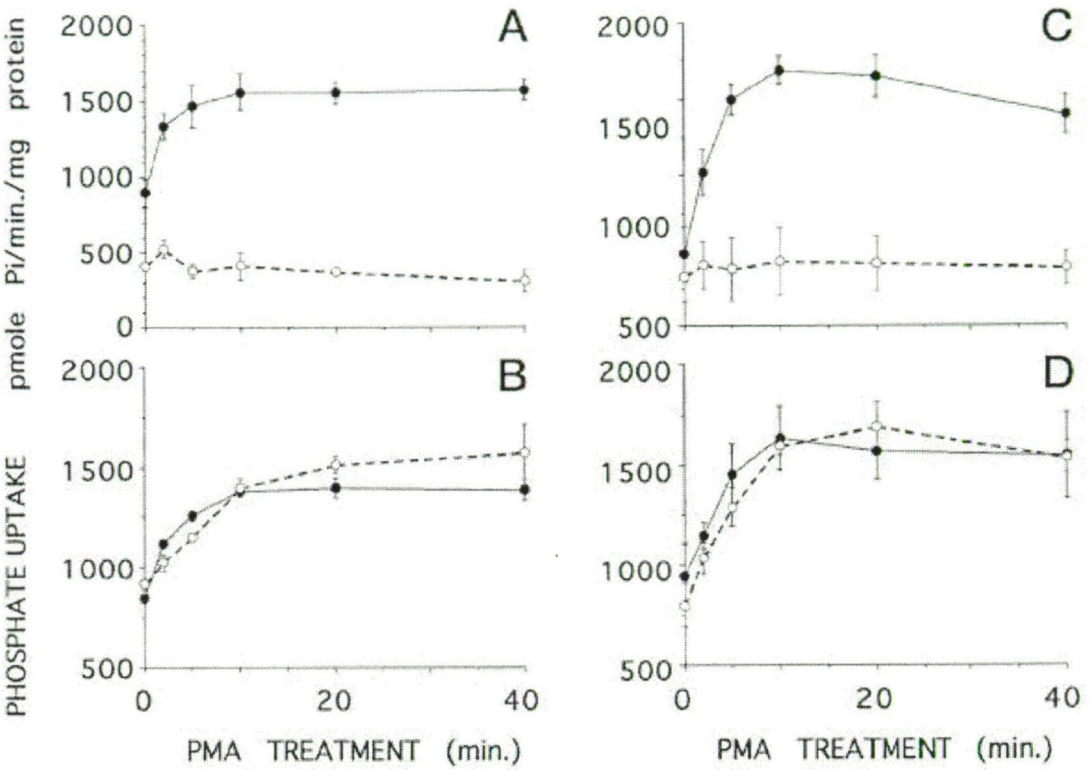

Figure 1. Effects of infection of cells with the amphotropic murine leukemia virus, the ecotropic murine leukemia virus, and the gibbon ape leukemia virus on the activation of sodiumdependent P_i uptake by PMA. NIH 3T3 cells were productively infected with wild type A-MuLV (*A*, ○) and E-MuLV (*B*, ○) and then treated with 1 μM PMA for the periods indicated. Mink fibroblasts were infected with wild type A-MuLV (*C*, ○) and wild type GALV-1 (*D*, ○) and then treated with 1 μM PMA for the times indicated. Uninfected cells were used as control for each experiment (●). P_i transport activity was determined as described under "Experimental Procedures." The data are given as the mean ± S.E. of two to four separate experiments each carried out in duplicate.

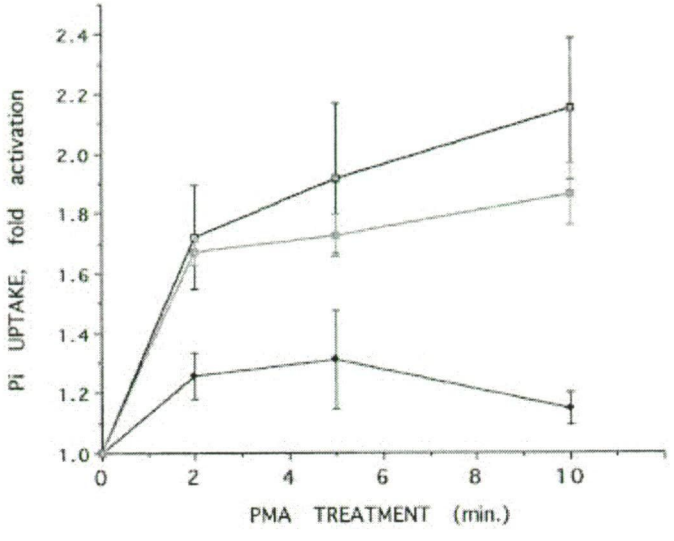

Figure 2. Effect of PKC inhibitors on the PMA-induced stimulation of P_i uptake. Serum-starved NIH 3T3 cells were preincubated with 0.01% dimethylsulfoxide as solvent control (□), 500 nM bisindolylmaleimide (♦), or 500 nM Gö 6976 (■) for 4 h, and then treated with 1 μM PMA for the times indicated. P_i transport activity was determined as described under "Experimental Procedures." Data represent the mean ± S.E. of three independent experiments performed in duplicate ($n = 6$). As determined by Student's t test, the inhibitory effects noted with bisindolylmaleimide were statistically significant ($p < 0.05$), whereas the slight effects noted with Gö 6976 ($p > 0.4$) were not significant.

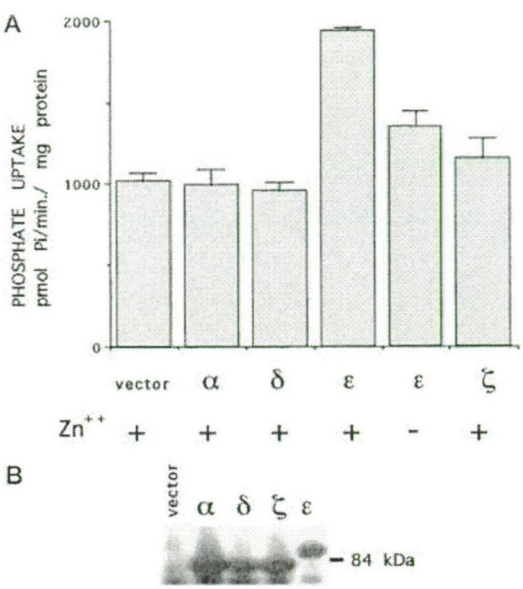

Figure 3. Effect of overexpression of different PKC isotypes on P_i uptake. *A*, vector control and PKC isotype overexpressor NIH 3T3 cells were serum starved for 24 h in the presence (+) or absence (−) of 20 μM zinc acetate. Short term (2-min) sodium-dependent P_i transport activity was determined in control and overexpressor cells as described under "Experimental Procedures." Each column represents the mean ± S.E. of three independent experiments performed in duplicate. *B*, Western blot analysis of the levels of $^{\varepsilon}$ epitope-tagged PKC isotypes in total cell extracts of the indicated PKC isotype overexpressor. NIH 3T3 cells were serum starved for 24 h in the presence of 20 μM zinc acetate, and total cell extracts then were prepared. Electrophoresis of total 20-μg protein lysate was carried out on 4-20% SDS-polyacrylamide gels, and immunoblot analysis was carried out with anti-$^{\varepsilon}$ epitope tag antibody as described under "Experimental Procedures."

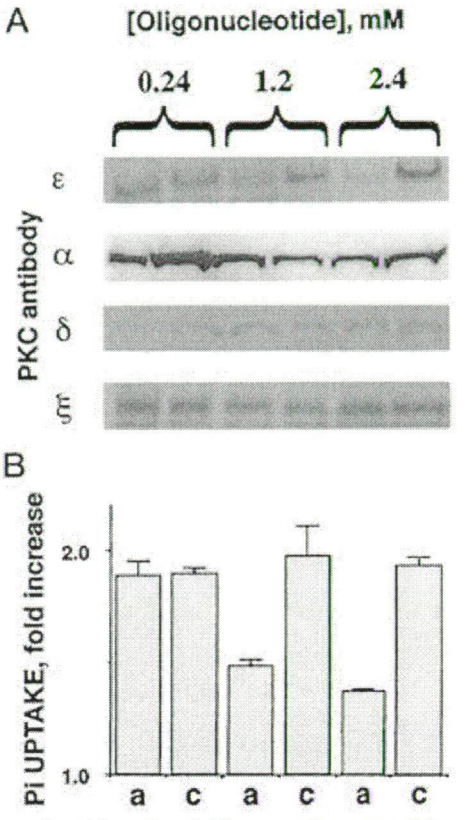

Fig. 4. Effect of PKCε-specific antisense oligonucleotide treatment of NIH 3T3 cells on PMA-induced stimulation of Na/P_i-uptake. The antisense (*a*) and scrambled control (*c*) oligonucleotides at the concentrations indicated were introduced into NIH 3T3 cells by electroporation, and the electroporated cells then were incubated for 24 h in the presence of the introduced oligonucleotides. *A*, selective decrease in PKCε protein levels with treatment of cells with PKCε-specific antisense oligonucleotides. Cells treated with the indicated concentrations of PKCε-specific antisense (*a*, ISIS 17260) or scrambled control (*c*, ISIS 17261) oligonucleotides for 24 h were harvested by scraping into lysis buffer. Aliquots of the cell lysates containing 100 μg of total protein were analyzed for changes in the levels of specific PKC isoforms by Western blotting using PKCε, α, δ and ζ izotype-specific antibodies. Western blot data represent a characteristic expression pattern of three similar experiments. *B*, treatment of NIH 3T3 cells with PKCε-specific antisense oligonucleotides inhibited the PMA-induced increase in P_i uptake. Cells treated with the indicated concentrations of oligonucleotides for 24 h were exposed to 0.01% dimethylsulfoxide (solvent control) or 1 μM PMA for 10 min, and short term P_i transport activity then was determined as described. Data are presented as the fold increase in P_i uptake in response to PMA treatment above basal values determined in the presence of dimethylsulfoxide. Results are given as the average ± S.E. of three separate uptake experiments performed in duplicate.

Figure 5. Functional and regulatory properties of recombinant human Pit-2 proteins Pit-2$^{\varepsilon\varepsilon}$ (A) and Pit-2-GFP (B). Short-term (2-min) P_i transport was determined in control p$^{\varepsilon}$MTH and pPit2$^{\varepsilon}$-$^{\varepsilon}$MTH-transfected NIH 3T3 fibroblasts as indicated in Materials and Methods. Cells were grown in serum-free medium with 20 μM zinc acetate to up-regulate the metallothionein promoter and then treated with 1 μM PMA for 10 min as indicated (C). (D) P_i uptake of p$^{\varepsilon}$MTH vector- and pPit2$^{\varepsilon}$-$^{\varepsilon}$MTH vector-transfected fibroblasts, as well as in these transfected cells productively infected with A-MuLV. Each column represents the mean ± standard error of the mean of three independent experiments performed in duplicate.

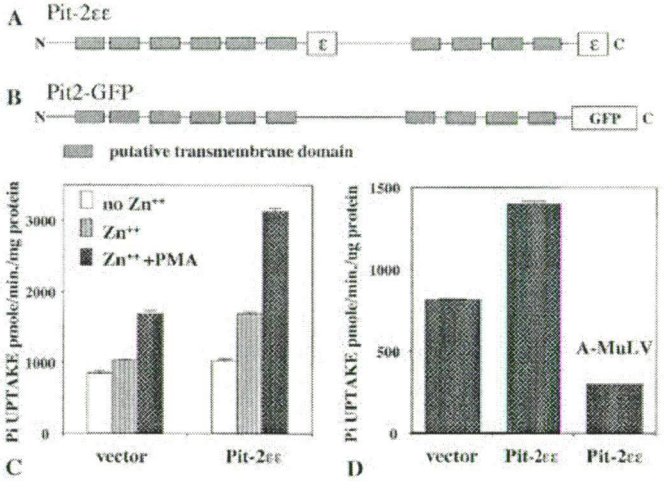

Figure 6. Western blot analysis of cell lysates prepared from $^{\varepsilon}$-epitope-tagged Pit-2 overexpressor fibroblasts productively infected with A-MuLV and E-MuLV. A 16,000 × *g* plasma membrane-enriched particulate fraction was prepared as described in Materials and Methods from control vector-transfected and Pit-2$^{\varepsilon\varepsilon}$ overexpressor fibroblasts, either uninfected or infected with A-MuLV or E-MuLV, as indicated. $^{\varepsilon}$-Tag antibodies (1:2,000) (A) and rabbit Pit-2 antiserum (1:500) (B) were used to detect Pit-2 in the particulate fraction of stable overexpressor cell lines. Closed arrows indicate Pit-2-specific bands in uninfected and E-MuLV-infected cells; open arrows indicate Pit-2 specific bands in A-MuLV-infected cells.

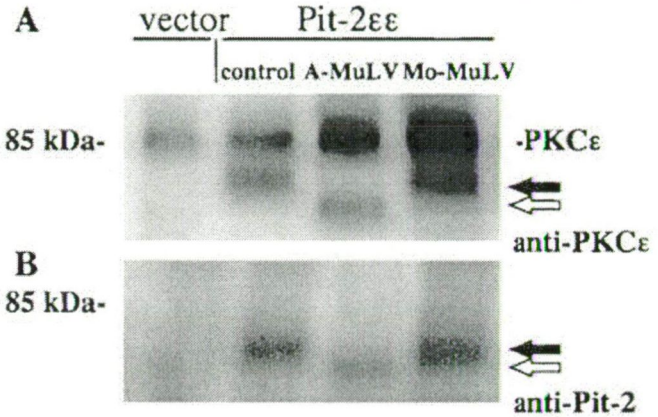

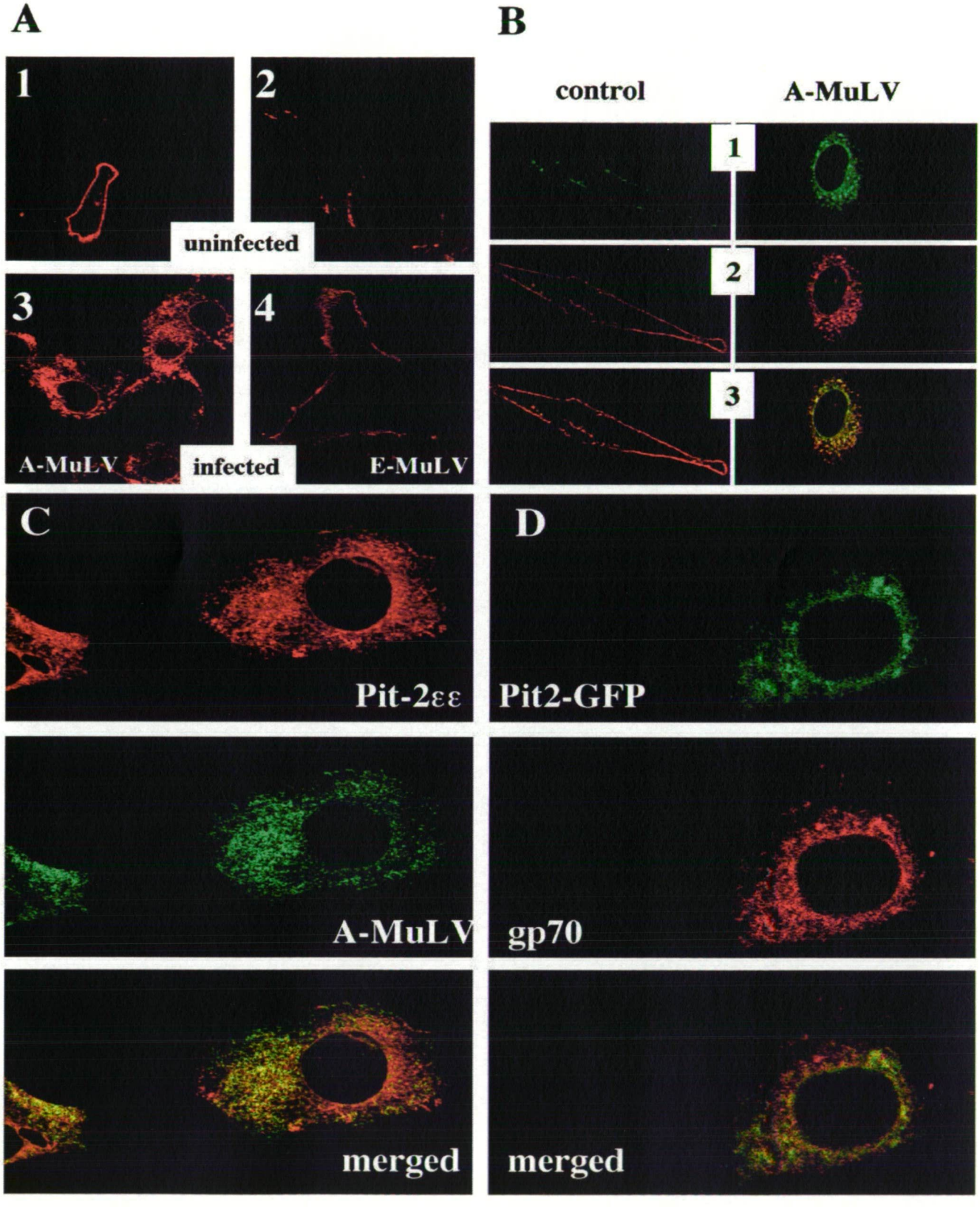
A
1
2
uninfected
3
4
A-MuLV
infected
E-MuLV
B
control
A-MuLV
1
2
3
C
Pit-2εε
D
Pit2-GFP
A-MuLV
gp70
merged
merged

Figure 7. Immunocytochemical localization of ε-epitope-tagged Pit-2 transporter in uninfected (A, 1and 2), and A-MuLV-infected (A, 3), and E-MuLV-infected (A, 4) overexpressor NIH 3T3 cells. ε-Tag antibodies (1:1,000 dilution) and Cy3-labeled anti-rabbit IgG (1:1,000 dilution) were used as primary and secondary antibodies, respectively, to stain for overexpressed Pit-2εε transporters. Views 1 and 2 in panel B depict dual imaging of control and A-MuLV-infected cells cooverexpressing both Pit-2-GFP chimeras and Pit-2εε, respectively. The coexpressed ε-epitope-tagged Pit-2 and the GFP-tagged Pit-2 were detected using fluorescent labeling and confocal laser microscopy as described in Materials and Methods. Panel C represents dual immunostaining of A-MuLV producer Pit-2εε-overexpressing NIH 3T3 fibroblasts with ε-tag antibodies and with A-MuLV pig antiserum. Cells were prepared and fixed on glass microscope slides as described in Materials and Methods. Pit-2εε staining with ε-tag antibodies was carried out as described in the legend to Fig. 6. The same cells were also stained for A-MuLV, using 1:500-diluted pig antiserum and 1:1,000-diluted fluorescein-conjugated anti-pig IgG secondary antibodies. Similarly stained uninfected and untransfected control NIH 3T3 cells were prepared to establish background levels for both the red and the green signals. Panel D shows A-MuLV-infected NIH 3T3 cells transiently transfected for 24 h with the pPit2-EGFPN1 construct and then stained for A-MuLV gp70 envelope protein with 1:500-diluted goat anti-Rausch murine leukemia virus gp69/71 antibody and 1:500-diluted Texas red-conjugated anti-goat IgG secondary antibodies. The distribution of Pit-2-GFP and A-MuLV gp70 protein was visualized under laser scanning confocal microscopy as described in Materials and Methods. The merged pictures of panels C and D resulted from merging the red and green signals.

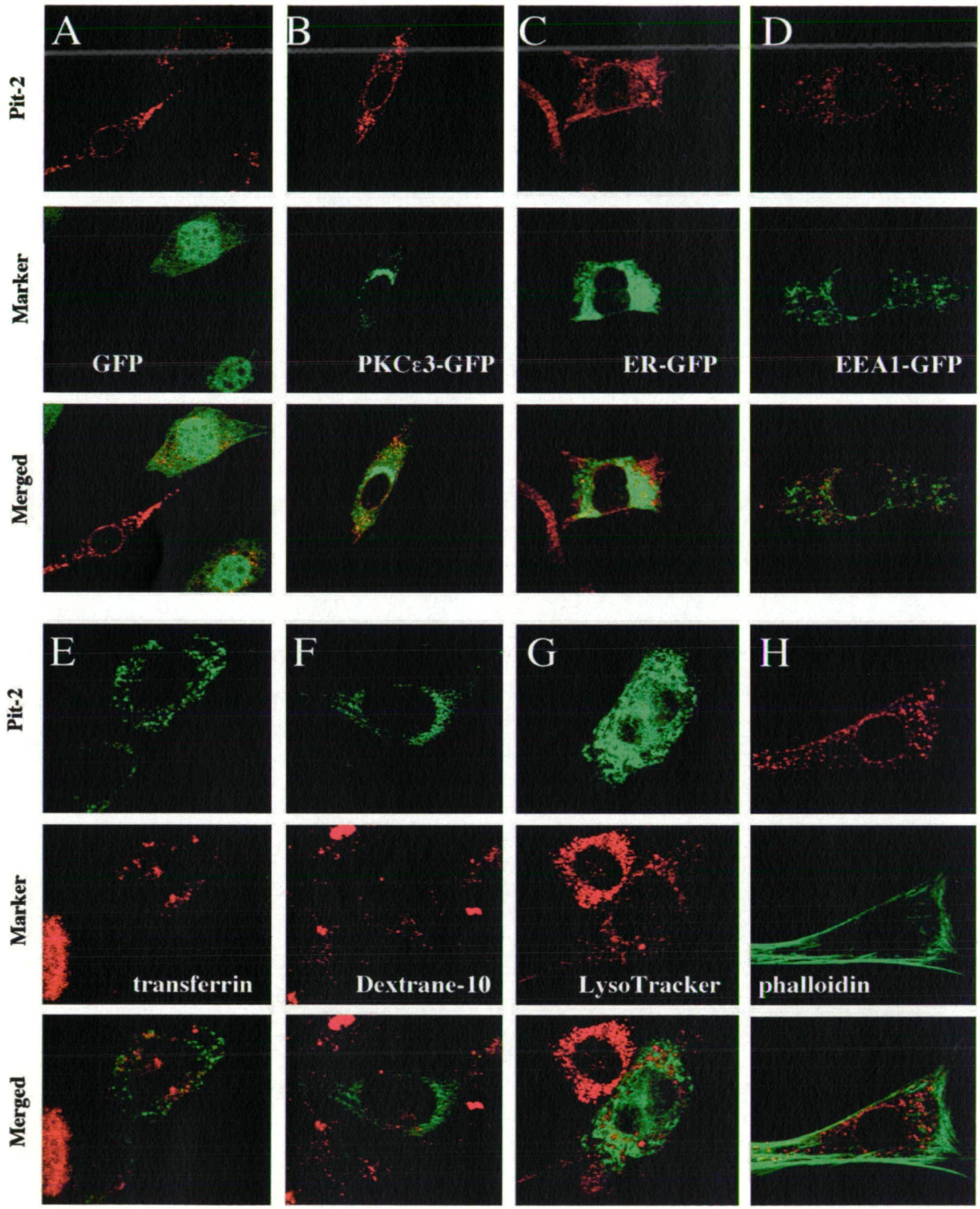
A
B
C
D
Pit-2
Marker
Merged
GFP
PKCε3-GFP
ER-GFP
EEA1-GFP
E
F
G
H
Pit-2
Marker
Merged
transferrin
Dextrane-10
LysoTracker
phalloidin

Figure 8. Dual immunostaining of overexpressed Pit-2 transporters with intracellular compartment markers in A-MuLV producer NIH 3T3 fibroblasts. A-MuLV producer, $^{\varepsilon}$-epitope-tagged Pit-2 overexpressor cells were transiently transfected with pEGFP-N1 (A), pPKC$^{\varepsilon}$3-EGFPC3 (Golgi-localizing chimera) (B), pER-GFP (coding for ER-targeted GFP) (C), and pEEA1-GFP (early endosome marker) (D), fixed, and stained with anti $^{\varepsilon}$-tag antibody as described in Materials and Methods. Alternatively A-MuLV-infected fibroblasts were transiently transfected with the pPit2-EGFP construct by electroporation and then labeled with transferrin (for recycling; endosomes) (E), dextran 10 (for late endosomes) (F), and LysoTracker (for lysosomes) (G) as detailed in Materials and Methods. A-MuLV producer, $^{\varepsilon}$-epitope-tagged Pit-2$^{\varepsilon\varepsilon}$ overexpressor cells were fixed and double stained with $^{\varepsilon}$-epitope antibody and fluorescein-conjugated phalloidin (for actin staining) (H). Control untransfected NIH 3T3 cells were prepared in the same manner to establish background levels for the $^{\varepsilon}$-tag antibody signal. Top panels within each experimental set represent Pit-2; middle panels represent different intracellular compartment markers within the same cells; lower panels show the results obtained with merging of the red and green signals.

Acknowledgement

I wish to thank Dr Wayne B. Anderson (LCO, NCI, NIH, Bethesda, USA) for his invaluable guidance with this project and the welcoming atmosphere he provided at the NIH. I also thank Prof. Erno Duda for his excellent mentoring and for his help with this thesis.

Appendix